To link to this article: DOI: 10.1016/j.camwa.2009.08.067

Simulation of fractionally damped mechanical systems by means of a Newmark-diffusive scheme

J.-F. Deü [a], D. Matignon [b,*]

[a] *Conservatoire National des Arts et Métiers (Cnam), Structural Mechanics and Coupled Systems Laboratory, Case 353, 292 rue Saint Martin, F-75141 Paris Cedex 03, France*

[b] *Université de Toulouse, ISAE, Applied Mathematics Training Unit, 10 avenue Edouard Belin, B.P. 54032, F-31055 Toulouse Cedex 4, France*

ARTICLE INFO

Keywords:
Fractional derivative
Diffusive representation
Viscoelasticity
Structural dynamics
Damping
Finite element method

ABSTRACT

A Newmark-diffusive scheme is presented for the time-domain solution of dynamic systems containing fractional derivatives. This scheme combines a classical Newmark time-integration method used to solve second-order mechanical systems (obtained for example after finite element discretization), with a diffusive representation based on the transformation of the fractional operator into a diagonal system of linear differential equations, which can be seen as internal memory variables. The focus is given on the algorithm implementation into a finite element framework, the strategies for choosing diffusive parameters, and applications to beam structures with a fractional Zener model.

1. Introduction

The importance of fractional calculus for modeling viscoelastic material behavior has been recognized by the mechanical scientific community since the pioneering work of [1]. The merits of using fractional differential operator lie in the fact that few parameters are needed to accurately describe the constitutive law of damping materials and the resulting model can be easily fitted to experimental data over a broad range of frequencies. The numerical approximation of such damped mechanical systems is today intensively studied with a special interest concerning the implementation of fractional constitutive equations into a finite element framework.

The resolution methods are classically either based on time discretization of the fractional dynamics (see e.g. [2–4]), or on diffusive representations (cf. [5–7]). For large scale systems, the first method proves memory consuming because it is necessary to store the whole displacement history of the system due to the non-local character of the fractional derivatives. The second method, based on diffusive realizations of fractional derivatives, is numerically more efficient because it has no hereditary behavior, thus avoiding the storage of the solution from all past time steps.

In this second group of methods, a coupled Newmark-diffusive scheme has recently been proposed by [8]. The developed algorithm has been analyzed through a single degree-of-freedom example and the numerical results have been compared to those obtained with an original closed-form solution. Here, we propose to extend our approach to more complex mechanical systems.

In this paper, the focus is given on the algorithm implementation compatible with finite element method, various strategies for choosing the diffusive parameters, and applications to beam structures.

* Corresponding author. Tel.: +33 5 61 33 81 12.
E-mail address: denis.matignon@isae.fr (D. Matignon).

2. Model under study

The main goal of this paper is to study fractionally damped oscillators using diffusive representations combined with a Newmark integration scheme. The equation of motion of N-degrees-of-freedom mechanical systems with fractional damping can be expressed as

$$\mathbf{M}\ddot{\mathbf{u}}(t) + \mathbf{C}\dot{\mathbf{u}}(t) + \mathbf{C}_\alpha(d^\alpha \mathbf{u})(t) + \mathbf{K}\mathbf{u}(t) = \mathbf{f}(t) \tag{1}$$

with appropriate initial conditions.

In (1) the mass, damping and stiffness matrices $\mathbf{M}$, $\mathbf{C}$, $\mathbf{C}_\alpha$ and $\mathbf{K}$ are symmetric and positive, $\mathbf{M}$ being positive *definite*. Moreover, for $0 < \alpha < 1$, $d^\alpha \mathbf{u} = I^{1-\alpha}\dot{\mathbf{u}}$ is the Caputo derivative of order $\alpha \in (0, 1)$, and $I^{1-\alpha}$ is the Riemann–Liouville fractional integral of order $1-\alpha$ defined by

$$I^{1-\alpha}\mathbf{v}(t) \coloneqq \frac{1}{\Gamma(1-\alpha)} \int_0^t \frac{1}{(t-\tau)^\alpha}\, \mathbf{v}(\tau)\mathrm{d}\tau. \tag{2}$$

where Γ is the Euler gamma function. When $\alpha = 1$, the classical damping term is defined separately $\mathbf{C}\dot{\mathbf{u}}$. For $1 < \alpha < 2$, $d^\alpha \mathbf{u}$ is understood as $d^{\alpha-1}\dot{\mathbf{u}}$.

3. A coupled Newmark-diffusive numerical scheme

3.1. Diffusive representation for fractional models

The diffusive representation is based on the following identity:

$$\forall t > 0, \quad \frac{1}{\Gamma(1-\alpha)}\, t^{-\alpha} = \int_0^\infty \frac{\sin\alpha\pi}{\pi} \frac{1}{\xi^{1-\alpha}} \mathrm{e}^{-\xi t}\mathrm{d}\xi, \tag{3}$$

which can be derived as follows: $\Gamma(\alpha) = \int_0^\infty x^{\alpha-1}\mathrm{e}^{-x}\mathrm{d}x = t^\alpha \int_0^\infty \xi^{\alpha-1}\mathrm{e}^{-t\xi}\mathrm{d}\xi$, thanks to the change of *positive* variables $x = t\,\xi$. The classical formula $\Gamma(\alpha)\Gamma(1-\alpha) = \pi/\sin(\alpha\pi)$ helps to recover the numerical coefficient in formula (3). The main advantage of this representation is that it allows the important interpretation: convolution by a fractional power-law is nothing but the continuous superposition of convolution by decaying exponentials (as solutions of first-order differential equations); the weight of this superposition is the function $\mu_{1-\alpha}(\xi) = \frac{\sin\alpha\pi}{\pi}\, \xi^{-(1-\alpha)}$ for $\xi > 0$.

We now study the two cases ($0 < \alpha < 1$ and $1 < \alpha < 2$) separately.

3.1.1. Standard case: $0 < \alpha < 1$

Following e.g. [5,6,9,10], letting $\mathbf{v} = \dot{\mathbf{u}}$, the term $d^\alpha \mathbf{u} = I^{1-\alpha}\mathbf{v}$ can be represented by a family of first-order systems indexed by $\xi > 0$:

$$\partial_t \boldsymbol{\varphi}(\xi, t) = -\xi\, \boldsymbol{\varphi}(\xi, t) + \mathbf{v}(t), \quad \boldsymbol{\varphi}(\xi, 0) = \mathbf{0}, \tag{4}$$

observed through the continuous superposition:

$$(I^{1-\alpha}\mathbf{v})(t) = \int_0^\infty \mu_{1-\alpha}(\xi)\boldsymbol{\varphi}(\xi, t)\mathrm{d}\xi, \tag{5}$$

where $\mu_{1-\alpha}(\xi) = \frac{\sin\alpha\pi}{\pi}\, \xi^{-(1-\alpha)}$.

The previous diffusive representation, which is *exact*, can be approximated by stable numerical schemes using standard *interpolation*, i.e.

$$\int_0^\infty \mu_{1-\alpha}(\xi)\boldsymbol{\varphi}(\xi, t)\mathrm{d}\xi \approx \sum_{k=1}^{K} \mu_k\, \boldsymbol{\varphi}(\xi_k), \tag{6}$$

where K is the number of approximation nodes, ξ_k a sequence of angular frequencies in the frequency range of interest, and μ_k the corresponding *interpolated* or *optimized* weights.

It is important to note that this finite-dimensional representation is only approximate and the quality of the approximation depends on the choice of these three parameters (see Section 5).

3.1.2. Extended case: $1 < \alpha < 2$

With the same family of first-order systems (4), we consider an extended observation as follows:

$$(d^{\alpha-1}\mathbf{v})(t) = \int_0^\infty \mu_{2-\alpha}(\xi)[\mathbf{v} - \xi\,\boldsymbol{\varphi}(\xi, t)]\mathrm{d}\xi, \tag{7}$$

where $\mu_{2-\alpha}(\xi) = \frac{\sin(2-\alpha)\pi}{\pi}\,\xi^{-(2-\alpha)}$.

As in the standard case, the extended diffusive representation is *exact*, and can be approximated by stable numerical schemes, such as:

$$\int_0^\infty \mu_{2-\alpha}(\xi)[\mathbf{v} - \xi\,\boldsymbol{\varphi}(\xi, t)]\mathrm{d}\xi \approx \sum_{k=1}^{K} \mu_k[\mathbf{v} - \xi_k\,\boldsymbol{\varphi}(\xi_k)], \tag{8}$$

but some care must be taken, see [7] for more technical details.

In particular, other possible discretizations would not respect discrete energy balances, which prove most useful in the stability analysis of coupled schemes, see chapter 3 of [11].

Note also that the density which is being used is $\mu_{2-\alpha}$ for the extended case, instead of $\mu_{1-\alpha}$ for the standard case.

3.2. Time-integration coupled scheme

Using the previous diffusive representation, a predictor–corrector algorithm based on the Newmark integration scheme (see e.g. chapter 9 of [12]) is proposed for the dynamic response of a fractionally damped system.

Some remarks can be made on the algorithm, which is detailed below:

- in the Newmark scheme, we use $\beta = 1/4$ and $\gamma = 1/2$ corresponding to the *average acceleration method*, which is unconditionally stable and second-order accurate for *non-dissipative* linear systems;
- the prediction velocity vector $\mathbf{v}_{\mathrm{pr}}$ is frozen as input of the diffusive sub-scheme 2(b).
- only the diffusive components $\boldsymbol{\varphi}_k^n$ for $1 \le k \le K$ at time step $n\Delta t$ are stored, but the previous vectors need not be stored ($\boldsymbol{\varphi}^{n-1}\ldots$).

---

1. Initialization
   $\mathbf{S} = \mathbf{M} + \gamma\,\Delta t\,\mathbf{C} + \beta\,\Delta t^2\,\mathbf{K}$
   $\mathbf{u}(0) = \mathbf{u}^0$, $\mathbf{v}(0) = \mathbf{v}^0$
   $\boldsymbol{\varphi}_k(0) = \mathbf{0}$ for $1 \le k \le K$
   $\mathbf{a}^0 = \mathbf{M}^{-1}(\mathbf{f}^0 - \mathbf{K}\,\mathbf{u}^0 - \mathbf{C}\,\mathbf{v}^0)$

2. Enter time step loop
   (a) Prediction
   $\mathbf{u}_{\mathrm{pr}}^{n+1} = \mathbf{u}^n + \Delta t\,\mathbf{v}^n + (0.5 - \beta)\Delta t^2\,\mathbf{a}^n$
   $\mathbf{v}_{\mathrm{pr}}^{n+1} = \mathbf{v}^n + (1 - \gamma)\Delta t\,\mathbf{a}^n$

   (b) Evaluation of $\boldsymbol{\varphi}_k^{n+1}$ for $1 \le k \le K$
   $\boldsymbol{\varphi}_k^{n+1} = \exp(-\xi_k\,\Delta t)\boldsymbol{\varphi}_k^n + \frac{1-\exp(-\xi_k\,\Delta t)}{\xi_k}\,\mathbf{v}_{\mathrm{pr}}^{n+1}$
   (c) Evaluation of $\mathbf{a}^{n+1}$
   Let $\boldsymbol{\theta}^{n+1} := \mathbf{f}^{n+1} - \mathbf{K}\mathbf{u}_{\mathrm{pr}}^{n+1} - \mathbf{C}\mathbf{v}_{\mathrm{pr}}^{n+1}$, then
   in **case** $0 < \alpha < 1$:
   $$\mathbf{S}\,\mathbf{a}^{n+1} = \boldsymbol{\theta}^{n+1} - \mathbf{C}_\alpha \sum_{k=1}^{K} \mu_k\,\boldsymbol{\varphi}_k^{n+1},$$
   or, in **case** $1 < \alpha < 2$:
   $$\mathbf{S}\,\mathbf{a}^{n+1} = \boldsymbol{\theta}^{n+1} - \mathbf{C}_\alpha \sum_{k=1}^{K} \mu_k\,[\mathbf{v}_{\mathrm{pr}}^{n+1} - \xi_k\,\boldsymbol{\varphi}_k^{n+1}].$$
   (d) Correction
   $\mathbf{u}^{n+1} = \mathbf{u}_{\mathrm{pr}}^{n+1} + \beta\,\Delta t^2\,\mathbf{a}^{n+1}$
   $\mathbf{v}^{n+1} = \mathbf{v}_{\mathrm{pr}}^{n+1} + \gamma\,\Delta t\,\mathbf{a}^{n+1}$

3. Update time step and return to step 2

---

4. A closed-form solution in fractional power series

In order to evaluate the efficiency of the previous algorithm, a closed-form solution has been developed for the following fractionally damped single degree-of-freedom (SDOF) equation:

$$m\ddot{u}(t) + c\dot{u}(t) + c_\alpha(d^\alpha u)(t) + \kappa\, u(t) = f(t) \tag{9}$$

with the initial conditions $u(0) = u^0$, $\dot{u}(0) = v^0$ and where $\alpha = \frac{p}{q} \in (0, 2)$, $p \wedge q = 1$.

The solution of (9) is proposed in three cases (in [4], only case (c) with $c = 0$ was studied):

(a) the free vibration due to an initial displacement:

$$f(t) \equiv 0, \qquad u^0 \neq 0, \qquad v^0 = 0;$$

(b) the free vibration due to an initial velocity:

$$f(t) \equiv 0, \qquad u^0 = 0, \qquad v^0 \neq 0;$$

(c) the dynamic response under a constant load:

$$f(t) = f^0 H(t), \qquad u^0 = v^0 = 0,$$

where H is the Heaviside function.

It can be noted that (b) and (c) correspond to impulse and step responses, respectively.

The key point is to write this exact solution in terms of fractional power series as

$$u(t) = \sum_{j=0}^{\infty} U_j\, t^{j/q} \tag{10}$$

where the jth coefficients U_j, obtained after some analytical calculations, are defined by:

- for $j \leq 2q$, the U_js are zero except the following:
  (a) $U_0 = u^0$, $U_{2q} = -\frac{\kappa}{2m}\, u^0$;
  (b) $U_q = v^0$, $U_{2q} = -\frac{c}{2m}\, v^0$;
  (c) $U_{2q} = \frac{1}{2m} f^0$;
- for $j > 2q$, the U_js are evaluated recursively by:

$$U_j = -\frac{1}{m}\frac{q^2}{j(j-q)}\left[\kappa\, U_{j-2q} + c\left(\frac{j-q}{q}\right) U_{j-q} + c_\alpha \frac{\Gamma\left(\frac{j+p-q}{q}\right)}{\Gamma\left(\frac{j-q}{q}\right)} U_{j+p-2q}\right].$$

Since u can be linearly decomposed into $2q$ Mittag-Leffler functions, see e.g. [5], and since the latter are entire functions, we know that the radius of convergence of the above series solution is infinite. In the sequel, it will be used to evaluate the accuracy of the Newmark-diffusive scheme for fractionally damped systems.

5. Strategies for choosing diffusive parameters

Based on Bode diagrams, a heuristic choice for the $\{\xi_k\}_{1\leq k\leq K}$ is given by a geometric sequence on a frequency range of interest.

Then, various choices are available for the $\{\mu_k\}_{1\leq k\leq K}$, see e.g. [6]. Let us give some more details on these choices and compare them on an example: only the standard case ($0 < \alpha < 1$) is considered in this section.

5.1. Interpolation method

We first focus on the *analytical* evaluation of μ_k, using the hat functions $\Lambda_k(\xi)$ of P_1-interpolation,

$$\Lambda_k(\xi) = \begin{cases} 0 & \text{if } \xi \leq \xi_{k-1} \text{ or } \xi \geq \xi_{k+1} \\ \dfrac{\xi - \xi_{k-1}}{\xi_k - \xi_{k-1}} & \text{if } \xi_{k-1} \leq \xi \leq \xi_k \\ \dfrac{\xi_{k+1} - \xi}{\xi_{k+1} - \xi_k} & \text{if } \xi_k \leq \xi \leq \xi_{k+1} \end{cases}$$

which gives

$$\begin{aligned} \mu_k &= \int_0^\infty \mu_{1-\alpha}(\xi)\Lambda_k(\xi)\mathrm{d}\xi \\ &= \frac{\sin\alpha\pi}{(1+\alpha)\alpha\pi}\left[\xi_{k+1}\left(\frac{\xi_{k+1}^\alpha - \xi_k^\alpha}{\xi_{k+1} - \xi_k}\right) - \xi_{k-1}\left(\frac{\xi_k^\alpha - \xi_{k-1}^\alpha}{\xi_k - \xi_{k-1}}\right)\right]. \end{aligned}$$

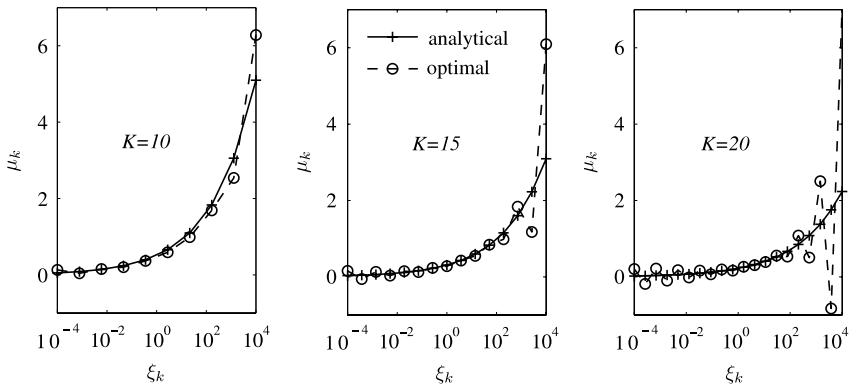

Fig. 1. Evolution of μ_k versus ξ_k $(1 \leq k \leq K)$ for $\alpha = 0.25$.

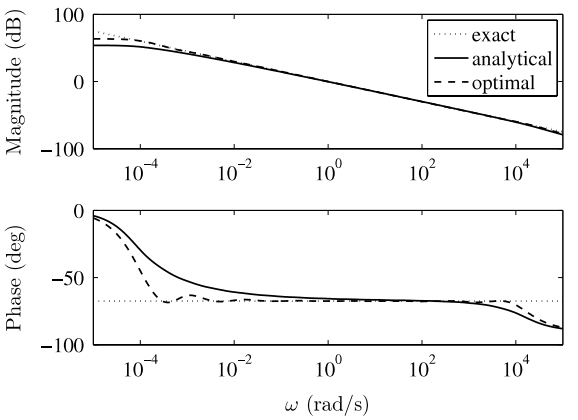

Fig. 2. Exact and approximated Bode plots for $\alpha = 0.25$: analytical and optimal ($K = 15$ and $\xi_k \in [10^{-4}, 10^4]$).

5.2. Optimization method

A second possibility consists in *optimizing* the μ_k with respect to a weighted (W_l) least-squares criterion, see e.g. [13]:

$$\mathcal{C}(\boldsymbol{\mu}) = \sum_{l=1}^{L} W_l \left| \sum_{k=1}^{K} \frac{\mu_k}{\mathrm{i}\omega_l + \xi_k} - \frac{1}{(\mathrm{i}\omega_l)^{(1-\alpha)}} \right|^2,$$

where $\{\omega_l\}_{1 \leq l \leq L}$ are angular frequencies, and $L \gg K$.

5.3. Comparison of the two methods on an example

Fig. 1 shows the analytical and optimal (with $L = 10\,K$ and $W_l = 1$) values of μ_k, for geometrically spaced ξ_k in $[10^{-4}, 10^4]$ and for $K = 10$, 15 and 20. We observe oscillations of the optimal μ_k around the analytical values, especially at the endpoints of the interval; even negative values can be found, which could be a problem for a further stability analysis.

The approximated Bode plots corresponding to $K = 15$ are shown in Fig. 2 and compared with the exact solution for which the magnitude behaves like $-6(1-\alpha)$ dB/oct and the phase is locked to $\mp(1-\alpha)\pi/2$ rad.

6. Analysis of the SDOF case

This section concerns the analysis of the Newmark-diffusive algorithm for the fractionally damped single degree-of-freedom equation. We consider the impulse response (cf. case (b) in Section 4) of Eq. (9) with the initial conditions $u^0 = 0$, $v^0 = 1$ and the mechanical parameters $m = 1, c = 0, c_\alpha = 0.5$ and $\kappa = 1$.

Fig. 3 presents the time displacement and the phase diagram for $\alpha \in (0, 1)$. One can observe the continuity of the behavior from the undamped ($\alpha = 0$) to the viscous case ($\alpha = 1$).

The closed-form solution presented in Section 4 is now used to evaluate the accuracy of the proposed algorithm. Note that a geometric sequence of ξ_k in conjunction with optimal values of μ_k ($K = 15, L = 10\,K$ and $W_l = 1$) are used in this analysis.

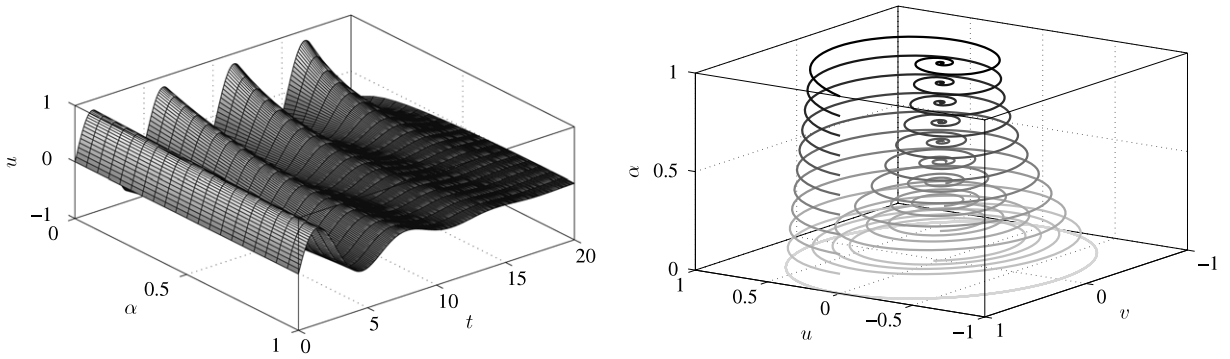

Fig. 3. Displacement versus time (left) and phase diagrams (right) for various fractional orders α. Case (b) with $v^0 = 1, m = 1, c = 0, c_\alpha = 0.5, \kappa = 1$.

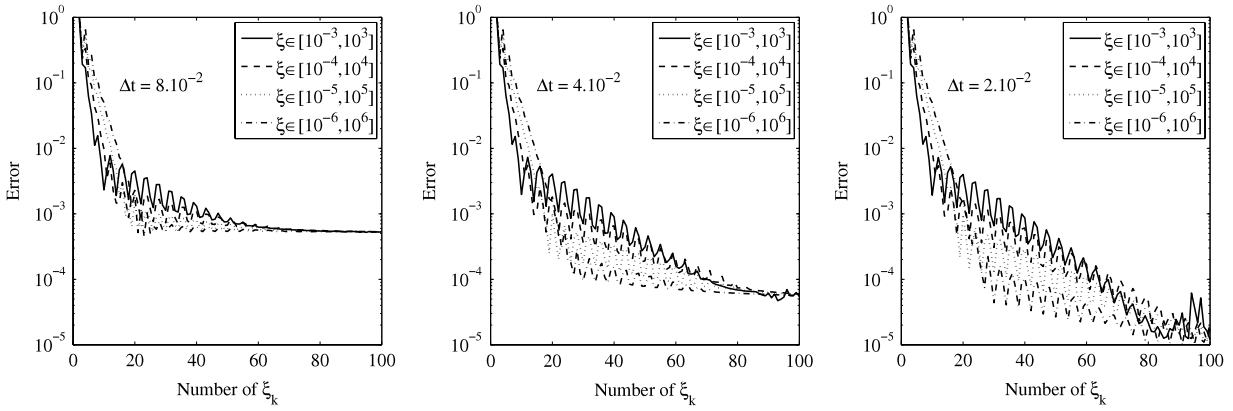

Fig. 4. Displacement error versus K (number of ξ_k) for four different ranges of frequencies and three time step size. Case (b) with $v^0 = 1, m = 1, c = 0$, $c_\alpha = 0.5, \kappa = 1$.

The displacement error for the SDOF with $\alpha = 0.25$ is presented in Fig. 4. These results show the influence of

1. the number of ξ_k,
2. the chosen frequency range of interest,
3. the time step size of the scheme.

From the results of the numerical experiments displayed in Fig. 4, the following points can be highlighted:

- for a given frequency range $[\xi_{\min}, \xi_{\max}]$, the slope of the error clearly changes for a particular value of K; oscillations occur in the second regime (due to the optimal choice of μ_k); eventually, a saturation of the error appears, which is due to the value of the time step (clearly observed in the case $\Delta t = 8 \times 10^{-2}$ for $K \geq 60$).
- for a given number K, the choice of frequency range $[\xi_{\min}, \xi_{\max}]$ which ensures the smallest error can be determined as follows: the smallest range $[10^{-3}, 10^{3}]$ has to be chosen while $K \lesssim 10$, and the biggest range $[10^{-6}, 10^{6}]$ has to be chosen when $K \gtrsim 25$; the optimal choice being less straightforward for $10 \leq K \leq 25$.
- a smaller time step gives a smaller asymptotic displacement error, as K increases, whatever the chosen frequency range.

Even if the previous comments pertain to case (b), the same kind of results can be derived for the two other cases (a) and (c), not shown here.

Note that at this stage, an error analysis is still to be carried out at a theoretical level, and will be investigated in future works. This will help define an optimal strategy in choosing the simulation parameters Δt, K, $[\xi_{\min}, \xi_{\max}]$.

7. Extension to viscoelastic beams

We propose here to extend our approach to a multi-degree-of-freedom system. The objective is to simulate the transient dynamic response of viscoelastically damped structures using the finite element method (FEM). As a first step, we consider a viscoelastic beam whose constitutive equation is defined in terms of fractional derivative operators.

7.1. Viscoelastic constitutive equations

The one-dimensional fractional Zener model is adopted to describe the behavior of the viscoelastic material

$$\sigma(t) + \tau^{\alpha}(d^{\alpha}\sigma)(t) = E_o\varepsilon(t) + E_{\infty}\tau^{\alpha}(d^{\alpha}\varepsilon)(t) \tag{11}$$

where σ and ε are the stress and the strain, E_o and E_∞ are the relaxed and non-relaxed elastic moduli, and τ is the relaxation time.

This four-parameter fractional derivative model has been shown to be an effective tool to describe the weak frequency dependence of most viscoelastic materials (see e.g. [1,14]).

After calculating the Fourier transform of Eq. (11), one obtains the expression of the elastic complex modulus

$$\widehat{E}(\omega) = \frac{\widehat{\sigma}(\omega)}{\widehat{\varepsilon}(\omega)} = \frac{E_o + E_{\infty}(\mathrm{i}\omega\tau)^{\alpha}}{1 + (\mathrm{i}\omega\tau)^{\alpha}} \tag{12}$$

where $\widehat{\sigma}$ and $\widehat{\varepsilon}$ are the Fourier transforms of $\sigma(t)$ and $\varepsilon(t)$, respectively. Its behavior in the frequency domain is described between two asymptotic values: the static modulus of elasticity $E_o = \widehat{E}(\omega \to 0)$ and the high-frequency limit value of the dynamic modulus $E_\infty = \widehat{E}(\omega \to \infty)$.

It is important to emphasize that the previous complex modulus has successfully been used to fit experimental data for a wide variety of materials, see e.g. [14].

7.2. Fractional Zener model as a diffusive model

The *causal* fractional Zener model defined by the frequency response (12) corresponds to the following transfer function in the Laplace domain:

$$\mathcal{E}(s) = \frac{E_o + E_{\infty}(\tau s)^{\alpha}}{1 + (\tau s)^{\alpha}} = \frac{E_o}{1 + (\tau s)^{\alpha}} + \frac{E_{\infty}}{1 + (\tau s)^{-\alpha}}, \tag{13}$$

at least in some right-half plane, $\Re e(s) \geq 0$, and we have $\mathcal{E}(\mathrm{i}\omega) = \widehat{E}(\omega)$.

Following the computations of diffusive representations for fractional differential systems, as introduced in [5], it is possible to find a diffusive representation for the E_0 part, and for the E_∞ part separately.

For the E_0 part, we compute (when $\tau = 1$):

$$\mu(\xi) = \frac{\sin(\alpha\pi)}{\pi} \frac{\xi^{\alpha}}{1 + 2\cos(\alpha\pi)\xi^{\alpha} + \xi^{2\alpha}}, \tag{14}$$

and for the E_∞ part, we compute (when $\tau = 1$):

$$\nu(\xi) = \frac{\mu(\xi)}{\xi} = \frac{\sin(\alpha\pi)}{\pi} \frac{\xi^{\alpha-1}}{1 + 2\cos(\alpha\pi)\xi^{\alpha} + \xi^{2\alpha}}. \tag{15}$$

Finally, we use the following identity:

$$\mathcal{E}(s) = E_0 \int_0^{\infty} \frac{1}{\tau s + \xi}\, \mu(\xi)\mathrm{d}\xi + E_{\infty} \int_0^{\infty} \frac{\tau s}{\tau s + \xi}\, \nu(\xi)\mathrm{d}\xi, \tag{16}$$

which we readily interpret as follows: the fractional Zener model (11)–(13) is a *positive* linear combination of

- a *standard* diffusive model w.r.t E_0 defined by positive density μ, given analytically by (14),
- an *extended* diffusive model w.r.t E_∞, defined by positive density ν, given analytically by (15).

This fundamental decomposition which, as far as we know, appears for the first time in this paper, proves that this model can be easily represented, analyzed and discretized, and that it fulfills *positivity* properties compatible with the second principle of thermodynamics, as already emphasized in [15]; to some extent, the *relaxation spectrum* and the *diffusive representation* are one but the same thing, up to a change of variables of the form $\xi = \tau^{-1}$: the main idea is that fractional derivatives can be transformed into *internal memory variable models*, the exact model possesses a continuum of memory variables $\boldsymbol{\varphi}(\xi, .)$ indexed by ξ, whereas any approximate model has finitely many memory variables, say $\boldsymbol{\varphi}(\xi_k, .)$ for $1 \leq k \leq K$.

7.3. Finite element considerations

For the sake of brevity, the finite element formulation is not presented in this paper. For details, the reader is referred to [3].

The discretized governing equation to be solved can be written is the following form

$$\mathbf{M}\ddot{\mathbf{u}}(t) + \mathbf{f}_{\text{int}}(t) = \mathbf{f}_{\text{ext}}(t) \tag{17}$$

where $\mathbf{M}$ is the mass matrix, $\mathbf{u}$ is the degrees-of-freedom vector, $\mathbf{f}_{\text{int}}$ and $\mathbf{f}_{\text{ext}}$ are the internal and external force vectors, respectively.

Note that the internal force vector is defined, at the elementary level, by

$$\mathbf{f}^{\text{e}}_{\text{int}}(t) = \int_{\Omega^{\text{e}}} \mathbf{B}^T \boldsymbol{\sigma}(t) \mathrm{d}\Omega \tag{18}$$

where $\mathbf{B}$ corresponds to the discrete strain–displacement operator (defined in terms of the derivatives of the shape functions), and $\boldsymbol{\sigma}$ contains the generalized stress components involved in the beam model (which are linked to the axial and shear strain – and consequently to the dofs – via the fractional derivative model (11)). Let us recall that, if the beam is elastic, this term is evaluated only once and is written $\mathbf{f}^{\text{e}}_{\text{int}} = \mathbf{K}^{\text{e}}\mathbf{u}^{\text{e}}$ where $\mathbf{K}^{\text{e}}$ is the elementary stiffness matrix and $\mathbf{u}^{\text{e}}$ the elementary degrees-of-freedom vector.

Here, due to fractional derivative constitutive equation of the viscoelastic beam, two strategies can be considered for the evaluation of the internal force vector at each time step of the Newmark time-integration method:

1. the first one, described in [3], consists of using a discrete time scheme for the fractional derivative (e.g. Grünwald–Letnikov approximation). This method implies the storage of the anelastic displacement variables on the whole history;
2. the second one, which is being used in this work, is based on the diffusive representation of the constitutive relation. In this case, the model is nothing but a *generalized Maxwell* viscoelastic constitutive equation whose material coefficients are directly linked to the diffusive parameters ξ_k and μ_k.

In the next subsection, some preliminary results are presented in order to show the potentialities of the method. Of course, further investigations will be needed to accurately compare the two previous approaches and show the better performance of the Newmark-diffusive scheme.

7.4. Preliminary results

Consider a viscoelastic cantilever beam of length $L = 150$ mm, width $b = 25$ mm and thickness $h = 5$ mm, discretized with 10 finite elements. The mechanical characteristics of the fictitious viscoelastic material are: mass density $\rho = 1000\ \text{kg/m}^3$, Poisson's ratio $\nu = 0.5$, relaxed elastic modulus $E_o = 1$ MPa, non-relaxed elastic modulus $E_\infty = 50$ MPa, relaxation time $\tau = 1$ ms and the fractional derivative order $\alpha = 0.5$.

The beam is subject to a transversal load at its free end such that

$$F(t) = \begin{cases} F_o t/t_1 & \text{for } 0 \le t \le t_1 \\ F_o & \text{for } t \ge t_1 \end{cases} \tag{19}$$

where $F_o = 0.01$ N, $t_1 = 50$ ms and simulation time $T = 1$ s. Additionally, for the Newmark scheme we use a constant time step $\Delta t = 2$ ms.

In Fig. 5, the transient responses of the damped viscoelastic beam are presented. The evolution of the tip displacement and the phase-space diagram are plotted in this figure. As expected, we observe that the oscillations of the viscoelastic beam are damped. It should be pointed out that these preliminary results show the versatility of the scheme since its implementation is easy and the numerical costs are greatly reduced compared to classical time discretization of the fractional derivatives.

8. Conclusion and perspectives

With this approach, complex mechanical systems with fractional damping can be efficiently simulated (in comparison to [3]) thanks to an appropriate finite element space discretization. As original example it is shown that the 4-parameter fractional Zener model fills in the framework of diffusive representations; and the positivity of the weights proves compatibility with the second law of thermodynamics.

Evaluation of the μ_k, which is a key point of the method, must be further investigated following the optimal approach. Moreover, a stability analysis of our coupled scheme has to be carried out, using energy balances, as fully detailed in [11]; moreover, specific discretization techniques, such as those developed in [7] which separate the local in time part from the historical part, could efficiently be implemented and further analyzed on our model.

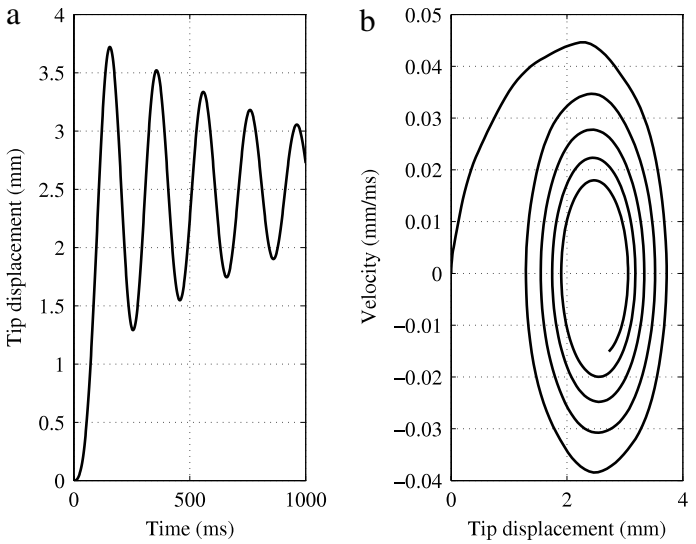

Fig. 5. Damped responses of the viscoelastic beam: (a) Tip displacement versus time; (b) Phase-space diagram.

Acknowledgement

The second author's work was supported by the CONSONNES project, ANR-05-BLAN-0097-01.

References

[1] R. Bagley, P. Torvik, Fractional calculus — A different approach to the analysis of viscoelastically damped structures, AIAA Journal 5 (5) (1983) 741–748.
[2] J. Padovan, Computational algorithms for FE formulations involving fractional operators, Computational Mechanics 2 (1987) 271–287.
[3] A. Galucio, J.-F. Deü, R. Ohayon, Finite element formulation of viscoelastic sandwich beams using fractional derivative operators, Computational Mechanics 33 (4) (2004) 282–291.
[4] A. Galucio, J.-F. Deü, S. Mengué, F. Dubois, An adaptation of the Gear scheme for fractional derivatives, Computer Methods in Applied Mechanics and Engineering 1995 (44–47) (2006) 6073–6085.
[5] D. Matignon, Stability properties for generalized fractional differential systems, in: ESAIM: Proceedings, vol. 5, 1998, pp. 145–158.
[6] D. Heleschewitz, Analyse et simulation de systèmes différentiels fractionnaires et pseudo-différentiels linéaires sous représentation diffusive, Ph.D. Thesis, ENST, 2000.
[7] H. Haddar, J.-R. Li, D. Matignon, Efficient solution of a wave equation with fractional order dissipative terms, Journal of Computational and Applied Mathematics (2009) 13, in press (doi:10.1016/j.cam.2009.08.051).
[8] J.-F. Deü, D. Matignon, A coupled Newmark-diffusive scheme for fractionnaly damped oscillators, in: Proceedings of the 8th International Conference on Mathematical and Numerical Aspects of Waves, WAVES 2007, INRIA, Reading, UK, 2007, pp. 526–528.
[9] D. Matignon, C. Prieur, Asymptotic stability of linear conservative systems when coupled with diffusive systems, ESAIM: Control, Optimisation and Calculus of Variations 11 (3) (2005) 487–507.
[10] D. Matignon, An introduction to fractional calculus, in: Scaling, Fractals and Wavelets (Digital Signal and Image Processing Series), ISTE–Wiley, 2008, 50 p. (Chapter 4).
[11] H. Haddar, D. Matignon, Theoretical and numerical analysis of the Webster–Lokshin model, Research. Rep. RR 6558, Institut National de la Recherche en Informatique et Automatique, INRIA, June 2008.
[12] T. Hughes, The Finite Element Method: Linear Static and Dynamic Finite Element Analysis, Prentice Hall, Englewood Cliffs, 1987.
[13] T. Hélie, D. Matignon, Representations with poles and cuts for the time-domain simulation of fractional systems and irrational transfer functions, Signal Processing 86 (10) (2006) 2516–2528.
[14] T. Pritz, Analysis of four-parameter fractional derivative model of real solid materials, Journal of Sound and Vibration 195 (1) (1996) 103–115.
[15] A. Lion, On the thermodynamics of fractional damping elements, Continuum Mechanics and Thermodynamics 9 (1997) 83–96.